

GAUSSIAN BEAM MODELING OF THE RADIUS OF CURVATURE

Kate M. Medicus¹, James Snyder¹, Angela D. Davies²

¹Department of Mechanical Engineering
Center for Precision Metrology
UNC Charlotte, Charlotte, NC

²Department of Physics and Optical Science
UNC Charlotte, Charlotte, NC

Abstract:

A Gaussian model of the radius measurement of micro-optics has been developed and tested using simulations. The model is based on the propagation distances in the interferometer, a heretofore uninvestigated effect. The goal of the model is to determine the bias error in the radius due to the Gaussian Beam propagation model. After testing the model with varying conditions, we have concluded the following: the measured part is smaller than the input, the cat's eye and confocal positions have approximately the same error, radius error increases with smaller test parts, decreasing the numerical aperture increases the errors, and the propagation distances do not affect the radius. The outline of the experimental plan to be used to verify the results is given.

1.0 Introduction

Micro-optic components are the key to building compact optoelectronic systems and are used in many applications such as optical networks, medical imaging, and optical data storage. These components have aperture diameters from 10 micrometers up to fractions of a millimeter. A crucial step in the manufacturing of the refractive micro-optic lenses is the measurement of the radius of curvature (ROC). The interferometric measurement of ROC is defined as the distance between the confocal reflection and the cat's eye retro-reflection [1, 2, 3]. The confocal position occurs when the optic is placed in the test beam of the interferometer such that the wavefront curvature of the incoming beam and the curvature of the test optic match. In the geometric model, the cat's eye position occurs when the surface of the optic is coincident with the focus of the test beam.

Traditionally, a geometric model of each position is used to describe the ROC measurement [1]. For micro-optics and high precision macro-optics, this model is not adequate to describe the ROC measurement. We believe a Gaussian beam propagation model is required and will offer lower ROC measurement uncertainty due to eliminating a systematic bias. This paper describes Gaussian beam approximations used to model the radius measurement and proposed experiments to validate the model.

2.0 The Radius Measurement

A schematic of the radius measurement is shown in Figure 1. The laser and collimating optics (not shown) produce a collimated beam with a well defined waist that enters the beam splitter where the light is split into two arms, the reference arm and test arm. In the reference arm, the beam propagates a distance of d_r , reflects off the reference mirror (labeled Ref. mirror) and again propagates a distance of d_r . In the test arm, the beam propagates a distance of d_t , is focused by a lens with focal length, f , propagates a distance s , reflects from the test optic with radius r , propagates a distance s , is collimated by a lens with focal length, f , and is propagated a distance d_t . At the beam splitter, the test and reference arms interfere and are focused onto the camera using imaging optics (not shown). Note that in Figure 1, the ray traces are shown to demonstrate the operation of the interferometer and do not indicate the Gaussian beam.

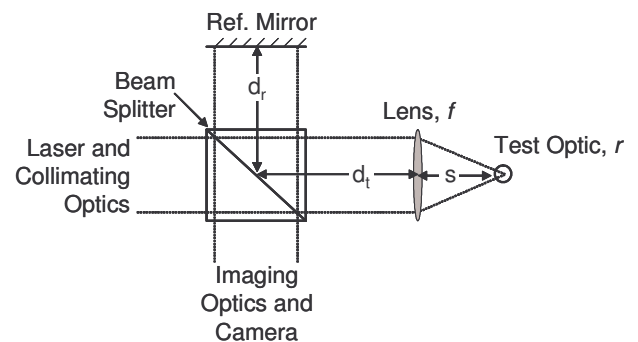


Figure 1: Radius measurement schematic.

3.0 The Gaussian Beam Model

A Gaussian beam can be described with a complex beam radius of curvature, q [4]:

$$\frac{1}{q} = \frac{1}{R} + i \frac{\lambda}{\pi w^2}$$

Equation 1,

where R is the radius of curvature of the wavefront and w the beam half width. The parameters R and w , and consequently the complex beam radius, are functions of position along the optical axis. That is, as the beam propagates in space (or through an optical system) the beam curvature and size change. The complex beam radius and the propagation of the beam through the optical system are used to model the radius measurement.

We can identify an input complex beam curvature as q_{in} (defined later). As the beam passes through each element in the optical system, the complex beam curvature changes. Each element is represented by a 2x2 matrix, M , in the traditional manner [5], as shown in Equation 2. The output beam complex radius of curvature, q_{out} [4], can be calculated in the following manner:

$$M = \begin{bmatrix} A & B \\ C & D \end{bmatrix} \quad q_{out} = \frac{Aq_{in} + B}{Cq_{in} + D}$$

Equation 2.

3.1 The Matrices

This section defines the matrix, M , which is used to model the interferometer. Each element in the test and references arms can be described using the matrix method of analysis. These elements are propagation, mirrors, and lenses. Equation 3 gives the equations for propagation through a distance d , M_{Prop} , a thin lens with focal length f , M_{Lens} , a mirror with radius r (the test optic), M_{Optic} , and the reference mirror (radius is infinite), M_{Mref} [5].

$$M_{Prop} = \begin{bmatrix} 1 & d \\ 0 & 1 \end{bmatrix} \quad M_{Lens} = \begin{bmatrix} 1 & 0 \\ -1/f & 1 \end{bmatrix}$$

$$M_{Optic} = \begin{bmatrix} 1 & 0 \\ 2/r & 1 \end{bmatrix} \quad M_{Mref} = \begin{bmatrix} 1 & 0 \\ 0 & 1 \end{bmatrix}$$

Equation 3.

Each arm of the interferometer is then represented by the multiplication of the matrices

of each element in the arm. The reference arm matrix, M_{ref} is propagation, reflection, and propagation as shown:

$$M_{ref} = \begin{bmatrix} 1 & d_r \\ 0 & 1 \end{bmatrix} \begin{bmatrix} 1 & 0 \\ 0 & 1 \end{bmatrix} \begin{bmatrix} 1 & d_r \\ 0 & 1 \end{bmatrix} = \begin{bmatrix} 1 & 2d_r \\ 0 & 1 \end{bmatrix}$$

Equation 4.

The matrix for the test arm, M_{test} is more complex with propagation by d_b , focusing by f , propagation by s , reflection at r , propagation by s , collimation by f , and propagation by d_t as shown:

$$M_{test} = \begin{bmatrix} 1 & d_t \\ 0 & 1 \end{bmatrix} \begin{bmatrix} 1 & 0 \\ -1/f & 1 \end{bmatrix} \begin{bmatrix} 1 & s \\ 0 & 1 \end{bmatrix} \begin{bmatrix} 1 & 0 \\ 2/r & 1 \end{bmatrix}^*$$

$$\begin{bmatrix} 1 & s \\ 0 & 1 \end{bmatrix} \begin{bmatrix} 1 & 0 \\ -1/f & 1 \end{bmatrix} \begin{bmatrix} 1 & d_t \\ 0 & 1 \end{bmatrix}$$

Equation 5.

The M_{ref} and M_{test} matrices are simplified and used in Equation 2 to calculate the output beam complex radius of curvature of the reference and test beams respectively, q_{rout} and q_{tout} . The parameter q_{tout} is a function of the position s (the propagation distance after the lens) while q_{rout} is constant and depends on the interferometer configuration.

4.0 The Confocal and Cat's Eye Positions

The confocal and cat's eye positions both occur when q_{rout} equals q_{tout} , that is, the interference pattern is flat. The reference arm q_{rout} is calculated using Equation 4 and Equation 2. and the test arm q_{tout} is calculated using Equation 5 and Equation 2. Since q_{tout} is a function of s and q_{rout} is constant there will be two positions where q_{rout} equals q_{tout} , each corresponding to a different value of s , one defining the cat's eye position and one defining the confocal position

The radius is then calculated as the difference between the cat's eye and confocal. It should be noted that this method requires defining q_{in} , the focal length of the lens, and the propagation distances, d_t and d_r . The nominal values for these parameters are based on the experimental setup. They are varied in simulation to study their effect on radius.

It should be noted that the propagation distances, d_t and d_r , can be set to provide for a perfect cat's eye and confocal reflections. However, the

propagation distances for the perfect cat's eye are not the same as for a perfect confocal. Obviously, moving either the reference mirror or the objective lens during the measurement is not feasible. Therefore a bias is introduced into the measurement. In addition, many of the required distances for perfect reflections are not practical (e.g. greater than 1 meter for a 100 μm part). Also, a precise measurement of the actual distance of the reference mirror and/or the lens can be prohibitively costly. Therefore, we will set the reference mirror and lens locations in the model using approximate values from our interferometer. We will study the effect of the position of these parts on the radius.

5.0 Determining the Inputs

The goal of this algorithm is to determine the error in the measured radius which changes with varying inputs like NA and part radius. The NA is changed in this model by varying the input beam complex radius of curvature, q_{in} . In the sections below, we describe two cases to calculate q_{in} and then the calculation of each of the remaining inputs.

5.1 Calculating q_{in} , Case 1

First we consider a standard interferometer with an aperture stop immediately before the beam splitter. The input beam is assumed to be collimated at this point and the aperture stop is overfilled such that the real part of the complex curvature goes to zero, that is, the beam is assumed to be flat at the stop. The complex q_{in} [4] for this case is

$$q_{in} = i \frac{\pi w^2 n}{\lambda}$$

Equation 6,

where w is the radius of the aperture stop, n the index of the medium (assumed to be 1) and λ is the wavelength of the incident light (a Helium-Neon laser at 632.8 nm). For an 8 mm diameter aperture stop (approximately equivalent to our micro-interferometer), q_{in} is $i*79393.17$ mm.

5.2 Calculating q_{in} , Case 2, and focal length

Another method to determine the input beam curvature is to work backwards from the focus point. This method assumes that the system is well designed and has a diffraction limited focus point. The inputs to this are the numerical aperture, NA, and the input beam diameter. The waist of a Gaussian beam at focus, w_0 , and the complex curvature at this point, q_0 [6], are given as

$$w_0 = \frac{\lambda}{\pi NA} \quad q_0 = i \frac{\pi w_0^2}{\lambda} = i \frac{\lambda}{\pi NA^2}$$

Equation 7.

We then use another matrix (not shown) with q_0 as the input beam curvature. This matrix travels from the focus point to the input of the beam splitter as shown in Figure 2. The output of this matrix calculation is q_{in} . The value for q_{in} is now a function of the NA, f , and d_t and is given as

$$q_{in} = d_t - f + i \frac{\pi NA^2 f^2}{\lambda}$$

Equation 8.

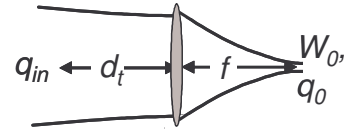


Figure 2: Schematic of Case 2, determining q_{in} .

The focal length, f , is calculated using the NA and the beam diameter. The calculated focal lengths for an input beam diameter of 8 mm and varying NAs are shown in Table 1. The NAs correspond to those of the microscope objectives used in our interferometer. The resultant q_{in} calculated using Equation 8 is also shown. The d_t parameter is adjusted based on the physical attributes of the micro-interferometer.

Table 1: The calculated f and q_{in} from the NA.

NA	f (mm)	q_{in} (mm) Case 2
0.28	13.7	dt - 13.7 + i*73206
0.42	8.6	dt - 8.6 + i*65421
0.55	6.1	dt - 6.1 + i*55405
0.70	4.1	dt - 4.1 + i*40511

5.3 The Remaining Inputs

We have shown two methods for determining the parameter q_{in} , as well as how to calculate the focal length based on the NA and the input beam size. The other relevant input parameters to be determined are d_t , d_r , and r . The distances in the test arm (d_t) and in the reference arm (d_r) are based on the range of the micro-interferometer, 50 mm to 100 mm and 150 mm to 300 mm, respectively. Finally r is defined by the test optics, and we are examining micro optics with radii ranging from 20 μm to 1 mm.

6.0 Obtaining Radius from the Model

Our goal is to determine the output radius of the test part and resultant error based on the input parameters described above. First, q_{in} and the focal length are calculated based on one of the methods described above. Next, q_{out} of the reference and test arms are calculated. A range of values are calculated for qt_{out} by varying s , taking care to encompass the both the cat's eye and confocal positions ($f-2r < s < f+r$). The curvature, $curv$, for both the reference and test arms is defined as the real part of the inverse of q_{out} and is given as

$$curv = \text{Re}\left(\frac{1}{q_{out}}\right) \quad \text{Equation 9.}$$

Note that $curv_{ref}$ has a single value for all positions and $curv_{test}$ is a function of s , the distance between the lens and the test part.

The cat's eye and confocal positions occur when the $curv_{test}$ and $curv_{ref}$ match. To do this, we define $curv_{out}$ as $curv_{test} - curv_{ref}$. The cat's eye and confocal positions occur at the s position where $curv_{out}$ is zero. An example graph of the $curv_{out}$ function is shown in Figure 3 with the confocal and cat's eye shown. The intermediate curve match near 9.47 mm is the result of unequal beam radii for q_{in} and q_{out} and is easily discarded as a solution.

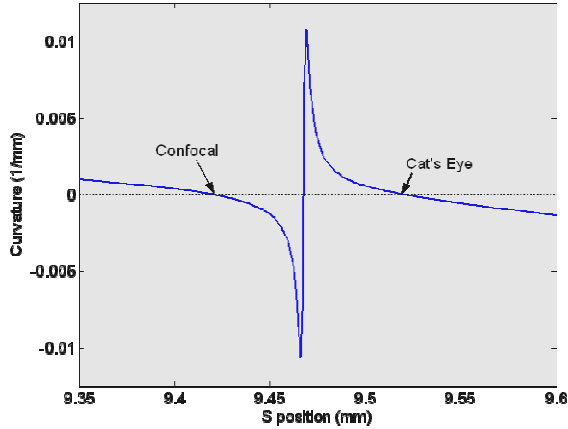


Figure 3: Example of a $curv_{out}$ function, $NA = 0.4$, $d_t = 100$ mm, $d_r = 150$ mm, $r = 100$ μ m, and $q_{in} = 90.48 + 71991i$ (Case 2).

The cat's eye and confocal positions were found by determining the s value where the function crossed the x-axis (in 0.1 nm sized steps) such that the position is certain to ± 0.1 nm. The radius

is then found by subtracting the confocal position, s_{CF} , from the cat's eye position, s_{CE} , and the radius error is computed:

$$\begin{aligned} Radius_{out} &= s_{CE} - s_{CF} \\ Radius_{error} &= Radius_{out} - r \end{aligned} \quad \text{Equation 10.}$$

The error is positive when $Radius_{out} > r$, input radius, and negative if the $Radius_{out} < r$. The offset of the cat's eye position is determined by subtracting the focal length of the lens from the s_{CE} position and the confocal offset is then found from the radius error and the CE_{offset} :

$$\begin{aligned} CE_{offset} &= s_{CE} - f \\ CF_{offset} &= Radius_{error} - CE_{offset} \end{aligned} \quad \text{Equation 11.}$$

By this convention, an offset toward the lens is negative and away is positive.

To summarize, the radius is found using the following steps:

- Calculate q_{in} and f
- Calculate qt_{out} (function of s) and qr_{out}
- Calculate $curv_{out}$ as a function of s
- Determine the two s positions where $curv_{out}$ is zero
- Radius is the difference between the two positions

7.0 Results of the Code

We are interested in testing the error in the radius of the test part as it depends on several parameters. The nominal values for these parameters are based on the experimental setup. They are varied in simulation to study their effect on radius. The results of the simulations are given in the sections below. The conclusions based on these results are in Section 7.4.

7.1 Varying Radius

We first tested parts with varying radius using the two different cases to determine q_{in} . For all these cases $d_t = 50$ mm, $d_r = 150$ mm, $\lambda = 632.8$ nm, the index of the air is 1, the NA is 0.42, the aperture size is 8 mm diameter, and the focal length is 8.6 mm. We are testing radius ranging from 0.02 mm to 1 mm as shown in the graphs below. Figure 4 and Figure 5 show the radius error when using q_{in} from Case 1 and 2, respectively.

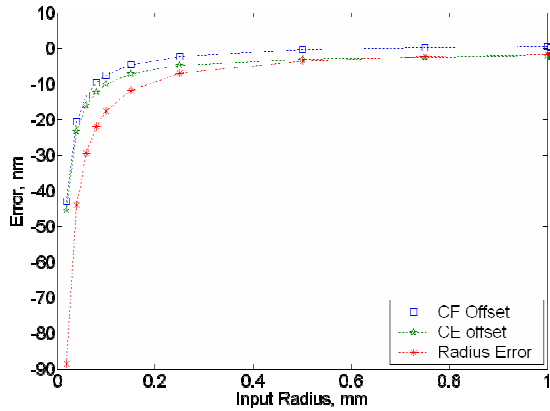


Figure 4: Radius Error for varying input radius using q_{in} from Case 1 ($q_{in} = 0 + 79433i$ mm).

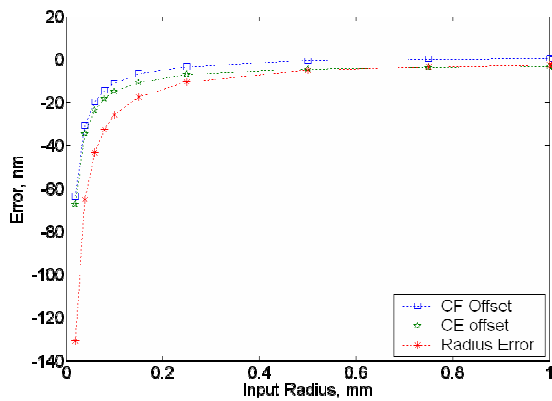


Figure 5: Radius Error for varying input radius, q_{in} from Case 3 ($q_{in} = 41.357 - 65421i$ mm).

7.2 Varying NA

Case 1, where q_{in} is calculated from the input beam diameter, is first considered. NA is varied, which affects the focal length of the lens. The input parameters are same as before and the NA ranges from 0.2 to 0.7. An input part radius of 500 μm was first tested and the results are shown in Figure 6.

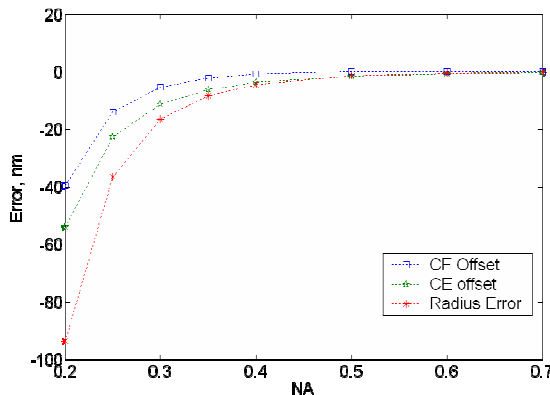


Figure 6: Radius Error for a 500 μm part, varying NA, q_{in} from Case 1.

Note that q_{in} does not change here; it is constant at $0 + 79433i$ mm, but the focal length does increase with decreased NA. Therefore, the radius error increases as focal length increases (decreasing NA). For a part radius of 250 μm , the trends are similar, but with a larger magnitude in error.

Determining the effect of NA on the part radius when using q_{in} from Case 2 is more complicated. This is because q_{in} is dependent on NA and focal length, which varies with NA. The distances d_t and d_r are the same as before and the input radius 500 μm . The results are shown in Figure 7.

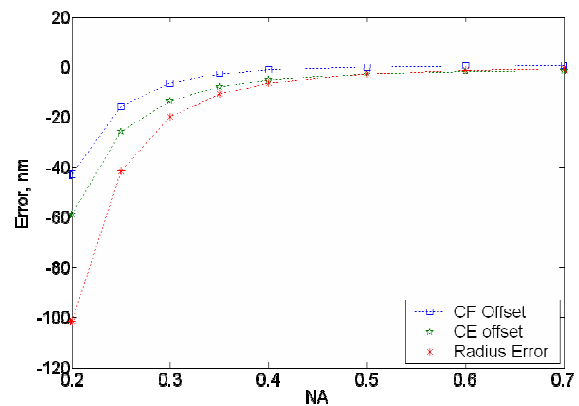


Figure 7: Radius Error in a 500 μm part, varying NA, q_{in} from Case 2.

This demonstrates the same trend as in Figure 6 and the errors are of the same magnitude, but the errors are not quite the same. This because the q_{in} changes with varying NA, unlike the previous case.

If the input radius is much smaller, 25 μm , the errors due to changing NA significantly increases to as much as 8% for a 0.2 NA.

7.3 Varying the propagation distances

The propagation distances, d_t and d_r were varied and the resultant errors examined. The results (not shown) indicate that the magnitude of the radius error is similar to previous results, but does not vary with changing d_t or d_r . However, the cat's eye and confocal positions do vary, but, the difference between the two is always the same. This is true regardless of the method to calculate q_{in} . Therefore, the propagation distance is not a factor in the radius measurement, but may be a factor in other types of interferometric measurements. For example,

propagation distance would matter if the measurement is absolute and not differential.

6.4 Conclusions about the model

From the results above and others not shown the following observations are made:

- The measured part is always smaller than the input radius.
- CE and CF offset errors are on the same order of magnitude.
- Radius error increases (apparently exponentially) as the radius decreases.
- Radius error increases (apparently exponentially) as NA decreases.
- Propagation distances d_t and d_r do not affect the radius measurement

It is interesting to note that decreasing the NA (equivalent to stopping the beam down) will increase the errors in the radius. Yet, often a beam is stopped down to reduce spherical aberration and therefore reduce a bias in the measurement due to the aberration.

8.0 Planned Experiments

Experiments are planned to verify the conclusions above using the Micro-Optics Transmission and Reflection Interferometer (MORTI) at UNC Charlotte. This interferometer, built on a microscope body, is a standard Twyman-Green, $\lambda = 632.8$ nm, with an objective lens as its focusing lens. A laser scale is used to measure the distance between the cat's eye and confocal positions. The laser scale is calibrated using a displacement measuring interferometer, not an artifact as with other interferometers. Additionally, MORTI is located in a temperature controlled metrology laboratory.

A series of steel spheres will be measured on MORTI with the following planned experiments:

- Varying the radius of the test part
- Using different objectives (NA)
- Stopping down the input beam
- Moving the reference mirror (d_r)

9.0 Future Plans

Further tests to be evaluated using the Gaussian beam model introduced in the paper include introducing aberrations and the Zernike defocus term to the model. The traditional radius measurement uses the Zernike defocus term to define the cat's eye and confocal positions [6], but the Gaussian beam model uses the $curv_{out}$

function. We predict these two methods will yield the same result in a non-aberrated system. But, in an aberrated system (typically spherical) we predict the results will not be the same.

The relationship between the $curv_{out}$ function and the Zernike defocus term must be evaluated. An optical path difference map can be generated at each s position from the $curv_{out}$ function. Then the Zernike polynomial fit must be performed to find the defocus term.

Spherical aberration can easily be added to the model using propagation through a glass plate in the converging beam. Different thickness of glass plate (equivalent to varying the aberration) will be tested. In general, we predict that the radius error will increase with increased aberration.

References

- [1] D. Malacara, Optical Shop Testing, 2nd Edition John Wiley & Sons, New York, 1992
- [2] T.L. Schmitz, C.J. Evans, A. Davies, and W.T. Estler, "Displacement Uncertainty in Interferometric Radius Measurements," *Annals of the CIRP*, Vol. 51, No. 1, p. 451-454, 2002
- [3] L. Selberg, "Radius measurement by interferometry," *Optical Engineering*, Vol. 31, No. 9, p. 1961-1966, 1992.
- [4] Yariv, Amnon, Optical Electronics, 4th Edition, Oxford University Press, New York, 1991.
- [5] F.L. Perrotti, and Perotti, L.S., Introduction to Optics, 4th Edition, Prentice Hall, NJ, 1993.
- [6] T.L. Schmitz, A. Davies, and C.J. Evans, "Uncertainties in interferometric measurements of radius of curvature", *Optical Manufacturing and Testing IV*, H. Stalh, Ed., *Proceedings of SPIE*, Vol. 4451, p. 432-447, 2001